



# Transitional character of Nd-Dy (N=90) isotones in IBM model

Abdullah H. Abd, Fahmi S. Radhi\*

Department of Physics, College of Education for Pure Sciences, University of Basrah, Basrah, Iraq.

## ARTICLE INFO

Received 03 July 2023  
Accepted 02 August 2023  
Published 30 December 2023

## Keywords :

IBM-1, energy levels, B(E2).

## ABSTRACT

The Interacting Boson Model is used to study the level structure of ground state, beta, and gamma bands in  $^{150}\text{Nd}$ ,  $^{152}\text{Sm}$ ,  $^{154}\text{Gd}$  and  $^{156}\text{Dy}$  (N = 90) isotones. The energy ratios  $R_{I+2/2}$  and  $R_{0_2/2_1}$  are compared to the predictions of U(5), SU(3), and X(5) symmetry. The calculated reduced transition probabilities as well as quadrupoles moments were compared to experimental data. IBM-1 investigates the properties of the potential energy surface to determine the nuclear shape of the Nd-Dy (N=90) isotones.

**Citation:** A. H. Abd, F. S. Radhi, J. Basrah Res. (Sci.) 49(2), 48 (2023).  
DOI: <https://doi.org/10.56714/bjrs.49.2.5>

## 1. Introduction

The Interacting Boson Model (IBM) was developed [1, 2] for describing collective excitations in medium and heavy mass nuclei. The IBM is based on the idea that collective excitations in atomic nuclei are described by bosons. The number of bosons is determined by the number of nucleon or hole pairs outside of a closed shell. These bosons can be classified into two types: s-bosons with angular momentum  $L = 0$  and d-bosons with  $L = 2$  [3, 4]. IBM-1 is the IBM model that does not distinguish between proton and neutron pairs, whereas IBM-2 explicitly introduces protons and neutrons. IBM-1 can be thought of as a quantized version of Bohr and Mottelson's collective model [5, 6]. The model's use of the symmetries of the boson operators introduced in the model is one of its advantages. The U(5), SU(3), and O(6) symmetries of the IBM-1 correspond to the spherical vibrator, deformed rotor, and  $\gamma$ -unstable nuclear structures, respectively [7-9]. The movement of nuclear shape from a vibrator to an axial rotor or to an  $\gamma$ -unstable rotor is referred to as the phase transition.

The movement of nuclear shape from a vibrator to an axial rotor or to an  $\gamma$ -unstable rotor is referred to as the phase transition. Iachello [10, 11] described the nucleus at the critical point of the U(5)-O(6) and U(5)-SU(3) transitional structures using the E(5) and X(5) symmetry. When there are few particles outside a closed shell of a nucleus, the pairing forces dominate, and the collective motion is a vibration about the spherical shape. The effect of longer-range forces becomes more noticeable as the number of

\*Corresponding author email : fahmishaban.fs@gmail.com





loose nucleons increases, and the nuclear shape becomes deformable. The isotones  $^{150}\text{Nd}$ ,  $^{152}\text{Sm}$ ,  $^{154}\text{Gd}$ , and  $^{156}\text{Dy}$  ( $N = 90$ ) have fewer neutrons outside the  $N = 82$  closed shell and are located away from the  $Z = 50$  closed shell, and are expected to have the  $U(5)$  to  $SU(3)$  transitional symmetry. Several experimental and theoretical studies have been conducted on the energy levels, electromagnetic transition probabilities, and potential energy surface of even-even rare-earth nuclei [12-17]. J. B. Gupta [18] used IBM-1 and the microscopic dynamic pairing plus quadrupole model to calculate energy levels and electric transition probabilities for  $^{146-152}\text{Nd}$ . The shape transition at  $N = 86-90$  was also explained using the microscopic dynamic pairing plus quadrupole model. Salah A. Eid and Sohair M. Diab [19] applied the IBM-1 to compute the excited positive and negative parity states, potential energy surfaces, and electromagnetic transition probabilities. The energy ratios and potential energy surface contour plots show that  $^{152}\text{Sm}$  is an  $X(5)$  candidate. Su Youn Lee et al. [20] used the  $U(5)$ - $SU(3)$  transitional symmetry for even-even nuclei in the Nd/Sm/Gd/Dy chains. The level structure and E2 transition probabilities were calculated. Hussein N. Qasim and Falih H. Al-Khudair [21] investigated the dynamic symmetry of the transitional nuclei  $^{140-154}\text{Nd}$ . The nucleus  $^{150}\text{Nd}$  is thought to have the properties of determination  $X(5)$ . HU Baoyue [22] calculated the energy levels and  $B(E2)$  for the even-even  $^{152-154}\text{Sm}$  to describe the  $U(5)$ - $SU(3)$  transitional symmetry for these nuclei using the IBM model. E.B. Balbutsev et al. [23] used the Wigner function moments (WFM) and QPNM methods to calculate energy levels,  $B(M1)$  transitions, scissor resonances, and the features of fine structure in  $^{148,150}\text{Nd}$ ,  $^{148,150,152,154}\text{Sm}$ ,  $^{156,158,160}\text{Gd}$ ,  $^{160,162,164}\text{Dy}$ . The results of the calculations were compared to experimental data. BC He et al. [24] investigated the transitional behaviour of the even-even  $^{144-156}\text{Nd}$  isotopes and came to the conclusion that the isotopes could be a good candidate for the first-order shape phase transition.

In the present work, the energy levels, transition probabilities  $B(E2)$ , quadrupole moments and Potential Energy Surface (PES) of the even-even  $^{150}\text{Nd}$ ,  $^{152}\text{Sm}$ ,  $^{154}\text{Gd}$  and  $^{156}\text{Dy}$  nuclei are studied within the IBM-1 model and the results are compared with the experimental data. The  $X(5)$  property for the Nd-Dy( $N=90$ ) isotones is investigated.

## 2. Calculations and results

### 1.1. Energy levels

The most popular IBM-1 Hamiltonian is given by [4]

$$\hat{H} = \varepsilon_d \hat{n}_d + a_0 \hat{P} \cdot \hat{P} + a_1 \hat{L} \cdot \hat{L} + a_2 \hat{Q} \cdot \hat{Q} + a_3 \hat{T}_3 \cdot \hat{T}_3 + a_4 \hat{T}_4 \cdot \hat{T}_4 \quad (1)$$

where  $\varepsilon$  is the d-boson energy, and the parameters  $a_0, a_1, a_2, a_3$  and  $a_4$  designate the strength of the pairing, angular momentum, quadrupole, octupole and hexadecapole interaction between bosons, respectively

The three dynamical symmetries of the IBM model are expressed as follow [26]

$$U(5): \hat{H} = \varepsilon \hat{n}_d + a_1 \hat{L} \cdot \hat{L} + a_3 \hat{T}_3 \cdot \hat{T}_3 + a_4 \hat{T}_4 \cdot \hat{T}_4 \quad (2)$$

$$SU(3): \hat{H} = a_1 \hat{L} \cdot \hat{L} + a_2 \hat{Q} \cdot \hat{Q} \quad (3)$$

$$O(6): \hat{H} = a_0 \hat{P} \cdot \hat{P} + a_1 \hat{L} \cdot \hat{L} + a_3 \hat{T}_3 \cdot \hat{T}_3 \quad (4)$$

In Eq. (3)

$$\hat{Q} = [d^\dagger \times \tilde{s} + s^\dagger \times \tilde{d}]^{(2)} + \chi [d^\dagger \times \tilde{d}]^{(2)} \quad (5)$$

where  $s^\dagger$  ( $\tilde{s}$ ) and  $d^\dagger$  ( $\tilde{d}$ ) are the creation (annihilation) operators for the  $s$  and  $d$  bosons.  $\chi$  is a shape parameter with values between 0 and  $\pm \frac{\sqrt{7}}{2}$

The  $^{150}\text{Nd}$ ,  $^{152}\text{Sm}$ ,  $^{154}\text{Gd}$  and  $^{156}\text{Dy}$  nuclei have eight neutrons more than the closed shell  $N = 82$ , with even proton numbers extended from 60 to 66 (away from the closed shell  $Z = 50$ ), resulting in a total boson number  $N$  ranging from 9 to 12. The values of the  $R_{4_1/2_1}$  ratio is plotted against proton number in Fig. 1 and presented in Table 1. It is appear that these isotones are having  $R_{4_1/2_1}$  ratio close to the

X(5) prediction 2.91. The X(5) symmetry is regarded as the critical point at which the U(5) - SU(3) phase transition occurs[11]. The IBM-1 energy level calculations have been carried out with PHINT code[29] . Table 2 displays the input parameter values that produce the best agreement with the experiment.

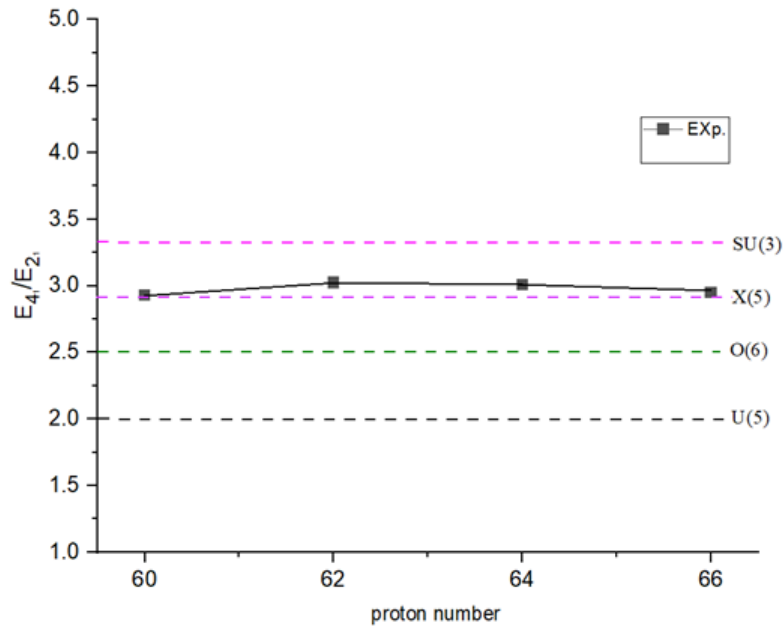


Fig.1 The experimental  $R_{4_1/2_1}$  ratio [30] of Nd-Dy (N=90) isotones compared with symmetry predictions

Table 1. The experimental [30] and symmetry values of  $R = \frac{E_{4_1^+}}{E_{2_1^+}}$

Isotone	$E_{4_1}/E_{2_1}$				
	Exp.	Symmetry			
		U(5)	O(6)	SU(3)	X(5)
$^{150}\text{Nd}$	2.930				
$^{152}\text{Sm}$	3.024				
$^{154}\text{Gd}$	3.008	2.00	2.50	3.333	2.91
$^{156}\text{Dy}$	2.948				

Table 2. The parameters of the IBM-1 Hamiltonian used for the descriptions of the  $^{150}\text{Nd}$ ,  $^{152}\text{Sm}$ ,  $^{154}\text{Gd}$ , and  $^{156}\text{Dy}$  isotones.

Isotones	N	EPS (Me V)	PAI R (Me V)	ELL (Me V)	QQ (Me V)	OC T (Me V)	HE X (Me V)	CH Q
$^{150}\text{Nd}$	9	0.46	0.01	0.00	-	0.00	0.00	-
		4	0	14	0.03	0	0	2.9
$^{152}\text{Sm}$	1	0.03	0.00	0.00	0.02	0.01	0.00	-
	0	0	0	90	47	50	35	2.9
$^{154}\text{Gd}$	1	0.37	0.00	0.01	-	0.00	0.00	-
	1	0	0	60	0.02	0	0	2.9
$^{156}\text{Dy}$	1	0.40	0.00	0.01	-	0.00	0.00	-
	2	0	0	40	0.02	0	0	2.9
					48			58

$\varepsilon = \text{EPS}$ ,  $a_0 = 2\text{PAIR}$ ,  $a_1 = 1/2 \text{ ELL}$ ,  $a_2 = 1/2 \text{ QQ}$ ,  $a_3 = 5 \text{ OCT}$  and  $a_4 = 5 \text{ HEX}$

The calculated IBM-1 levels for the ground state, beta, and gamma bands are shown in Fig. 2 along with the corresponding experimental data. The theoretical results in the figure agree well with the experimental ones for the nuclei under consideration. The IBM predictions, however, deviate from the experiment for the levels  $14_2^+$  and  $11^+$  in  $^{152}\text{Sm}$ ,  $12_1^+$  and  $10_2^+$  and in  $^{154}\text{Gd}$ , and  $14_1^+$  and  $11^+$  in  $^{156}\text{Dy}$ , with calculated energy values up to 650 KeV higher than the experimental data. The experimental levels denoted by '( )' are those whose spin and/or parity are uncertain.

The energy ratio  $R_{I+2/2}$ , for the  $I_i = 0_1^+, 2_1^+, 4_1^+, 6_1^+$  and  $8_1^+$  levels, of the yrast band for the Nd-Dy ( $N = 90$ ) isotones is plotted in Fig. 3, along with the U(5), SU(3), and X(5) predictions. The theoretical and experimental values of energy ratio  $R_{I+2/2}$  for these isotones, as shown in the figure, are associated with X(5) predictions for the yrast energy spacings, which are intermediate between the vibrational and rotational structures. Fig. 4 shows a good description of the energy ratio  $R_{0_2/2_1}$  for the IBM prediction with experiment and X(5) symmetry..

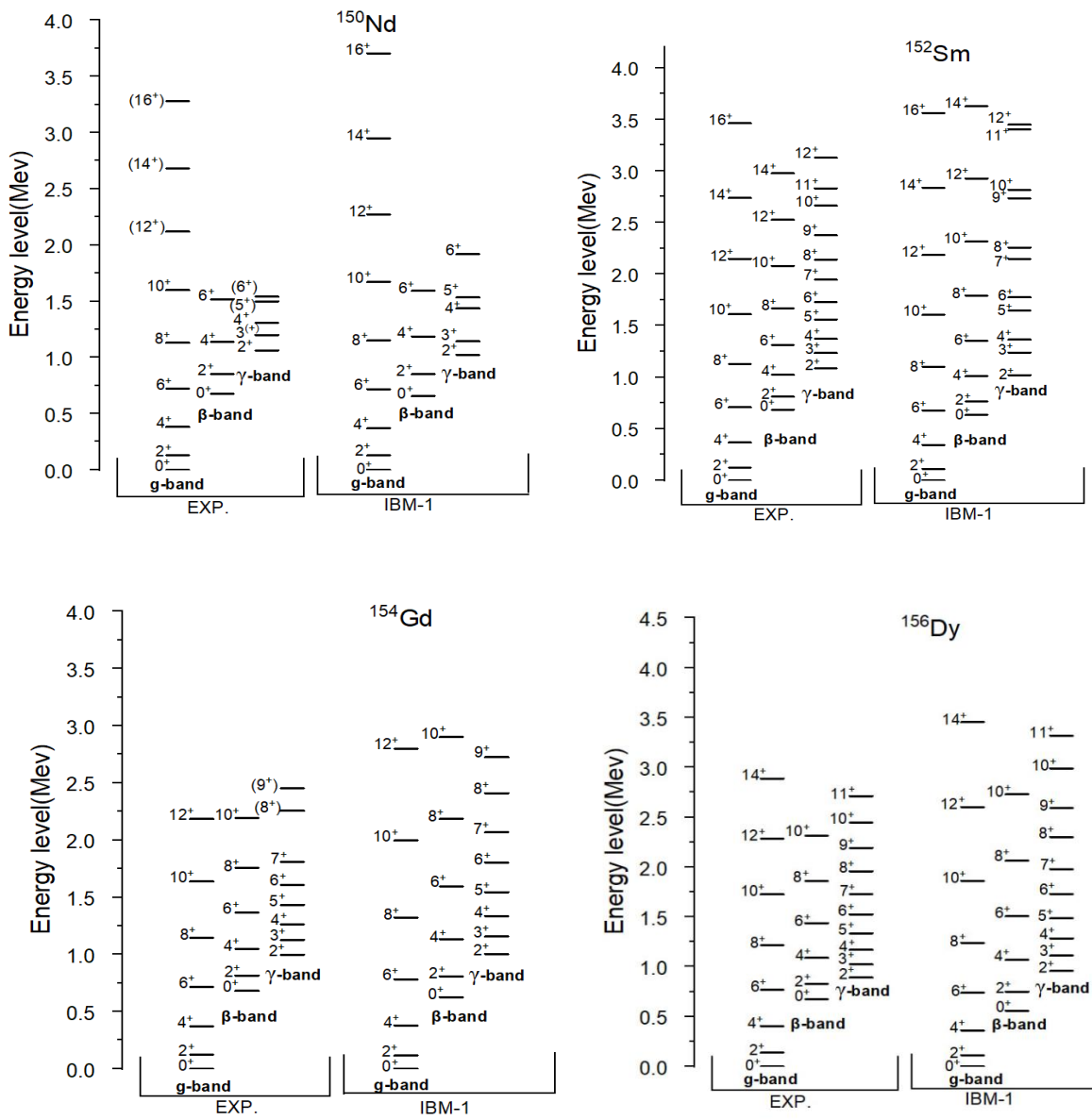


**Fig. 2.** Energy states of Nd-Dy isotones from IBM calculations in comparison with the experimental levels[30].

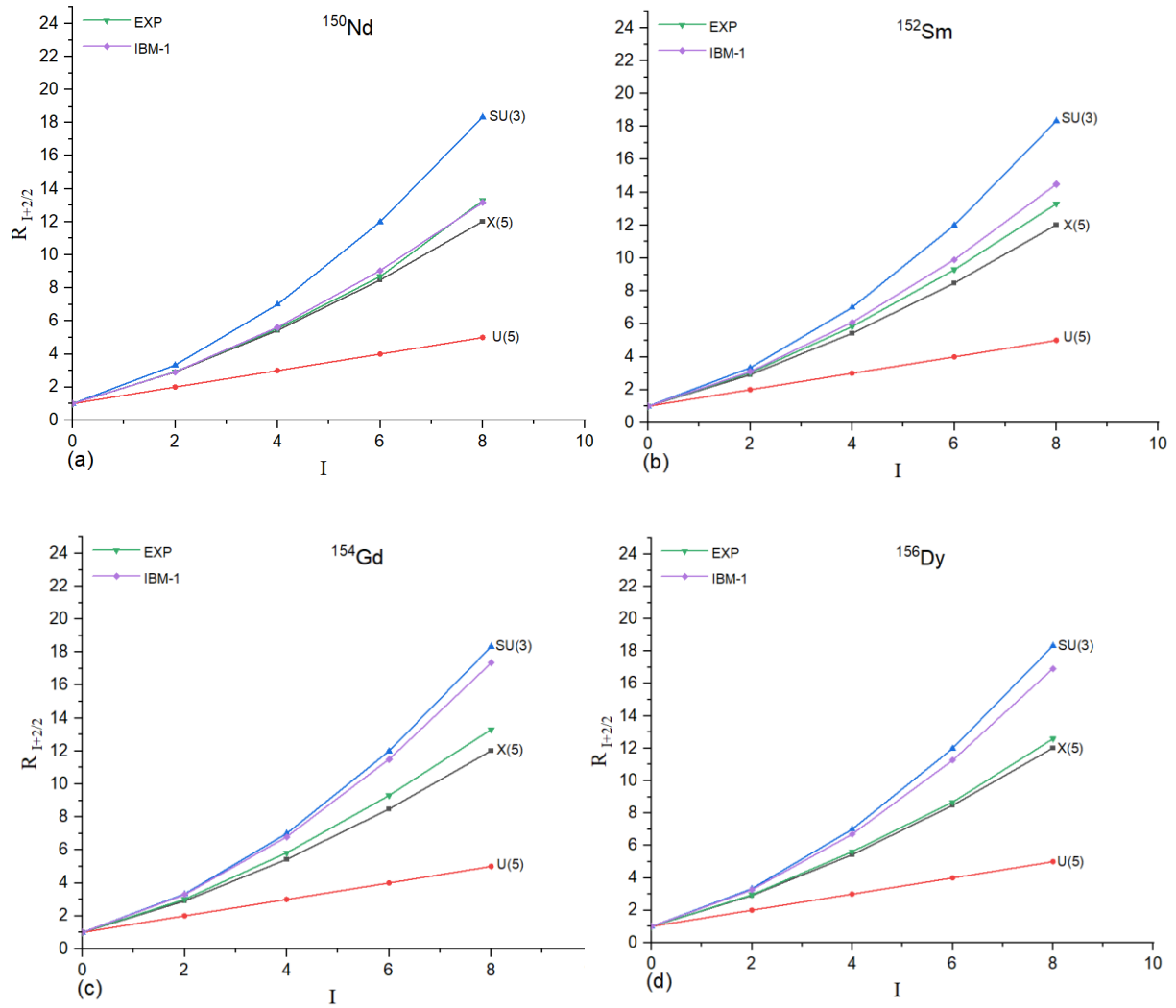


**Fig.3.** The energy ratio  $R_{I+2/2}$  of  $^{150}\text{Nd}$  (a),  $^{152}\text{Sm}$  (b),  $^{154}\text{Gd}$  (c), and  $^{156}\text{Dy}$  (d) isotones compared with symmetry predictions

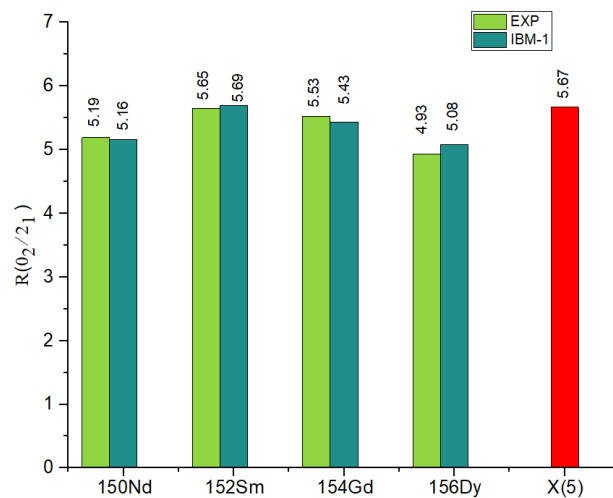


**Fig.4.** The energy ratio  $R_{0_2/2_1}$  of Nd-Dy(N=90) isotones in comparison with X(5) predictions.

### 1.2. Reduced transition probabilities

The electric quadrupole transition operator in IBM-1 takes the form [2, 7]:

$$T_m^{E2} = \alpha_2 [d^\dagger \times \tilde{s} + s^\dagger \times \tilde{d}]_m^2 + \beta_2 [d^\dagger \times \tilde{d}]_m^2 \quad (6)$$

$\alpha_2 = e_B$  is the boson effective charge and  $\beta_2 = \chi \alpha_2$ .

The reduced transition probabilities were calculated using the FBEM program [29]. The experimental  $B(E2; 2_1^+ \rightarrow 0_1^+)$  transition was used to normalize the values of the input parameters listed in Table 3.

Table 3. The boson effective charges used for B(E2) calculations.

Isotones	E2SD= $\alpha_2$	E2DD= $\sqrt{5}\beta_2$
<sup>150</sup> Nd	0.145	-0.368
<sup>152</sup> Sm	0.134	-0.392
<sup>154</sup> Gd	0.132	-0.383
<sup>156</sup> Dy	0.130	-0.300

Tables 4 and 5 display the calculated B(E2) values. The tables show that the B(E2) values for ground state band transitions increase with increasing proton number for the <sup>150</sup>Nd, <sup>152</sup>Sm and <sup>154</sup>Gd nuclei and then decrease when moving to the <sup>156</sup>Dy nucleus. The predicted B (E2) values and experimental data are generally in agreement. However, because the predicted interband transitions are governed by dynamical symmetry selection rules, weak B (E2) values are expected. Tables 4 and 5 also include the predicted values of electric quadrupole moments  $Q_{2_1}$  ; the agreement with the experiment is very good, both in sign and magnitude.

Table 4. Experimental B(E2) ( $e^2b^2$ ) values in the <sup>150</sup>Nd and <sup>152</sup>Sm nuclei compared with IBM predictions.

$I_i^+ \rightarrow I_f^+$	<sup>150</sup> Nd		<sup>152</sup> Sm	
	EXP[30]	IBM-1	EXP[30]	IBM-1
2 <sub>1</sub> →0 <sub>1</sub>	0.5493(142)	0.5509	0.6990(771)	0.7464
4 <sub>1</sub> →2 <sub>1</sub>	0.8547(16)	0.8154	1.0097(106)	1.0524
6 <sub>1</sub> →4 <sub>1</sub>	0.9743(425)	0.8982	1.1570(192)	1.1201
8 <sub>1</sub> →6 <sub>1</sub>	1.0216(1087)	0.9056	1.4125(192)	1.1034
10 <sub>1</sub> →8 <sub>1</sub>	0.9507(520)	0.8590	1.5137 ( <sup>1687</sup> <sub>1253</sub> )	1.0348
12 <sub>1</sub> →10 <sub>1</sub>	0.8182( <sup>1371</sup> <sub>946</sub> )	0.7667		0.9276
14 <sub>1</sub> →12 <sub>1</sub>		0.6327		0.7897
16 <sub>1</sub> →14 <sub>1</sub>		0.4593		0.6258
0 <sub>2</sub> →2 <sub>1</sub>	0.2038(23)	0.1868	0.1605(57)	0.0286
2 <sub>2</sub> →0 <sub>2</sub>	0.7568(614)	0.2217	0.8195(578)	0.5327
2 <sub>2</sub> →0 <sub>1</sub>	0.0033(23)	0.0027	0.0045(28)	0.0014
2 <sub>2</sub> →2 <sub>1</sub>	0.0473(141)	0.0655	0.0274(92)	0.0089
2 <sub>2</sub> →4 <sub>1</sub>	0.0898(331)	0.0237	0.0867(578)	0.0110
4 <sub>2</sub> →2 <sub>2</sub>	0.1087(376)	0.3986	1.2052(192)	0.7493
4 <sub>2</sub> →2 <sub>1</sub>	0.0007(0)	0.0001	0.0037(5)	0.0026
4 <sub>2</sub> →4 <sub>1</sub>		0.0501	0.0241( <sup>482</sup> <sub>337</sub> )	0.0100
4 <sub>2</sub> →6 <sub>1</sub>	0.0435(22)	0.0151	0.0819(144)	0.0072
2 <sub>3</sub> →0 <sub>2</sub>		0.1407	0.0001(0)	0.0009
			0.00081(10)	
			0.0012	
2 <sub>3</sub> →0 <sub>1</sub>	0.0141(283)	0.0113	0.0139(19)	0.0014
2 <sub>3</sub> →2 <sub>1</sub>	>0.0137	0.0004	0.0356(48)	0.0245
2 <sub>3</sub> →4 <sub>1</sub>	0.0080(12)	0.0580	0.0027(3)	0.0015



$3_1 \rightarrow 2_3$		0.4052	$0.5785 \binom{289}{433}$	0.8255
$3_1 \rightarrow 2_1$		0.0176	$0.0327 \binom{72}{53}$	0.0025
$3_1 \rightarrow 4_1$		0.0231	$0.0347 \binom{77}{53}$	0.0229
$4_3 \rightarrow 2_3$	0.6156(236)	0.3514		0.3075
$4_3 \rightarrow 2_1$	0.0027(9)	0.0035		0.0012
$Q_{2_1}$	-2.0(5)	-1.506	-1.683(18)	-1.738

Table 5. Experimental B(E2) ( $e^2b^2$ ) values in  $^{154}\text{Gd}$  and  $^{156}\text{Dy}$  nuclei compared with IBM predictions.

$I_i^+ \rightarrow I_f^+$	$^{154}\text{Gd}$		$^{156}\text{Dy}$	
	EXP[30]	IBM-1	EXP[30]	IBM-1
$2_1 \rightarrow 0_1$	0.7700(49)	0.7945	0.7486(848)	0.7872
$4_1 \rightarrow 2_1$	1.2017(441)	1.1336	1.2217(119)	1.1342
$6_1 \rightarrow 4_1$	1.3979(735)	1.2323	1.3175(648)	1.2471
$8_1 \rightarrow 6_1$	1.5303(8338)	1.2513	1.4024(399)	1.2833
$10_1 \rightarrow 8_1$	1.7658(196)	1.2199	1.5471(149)	1.2711
$12_1 \rightarrow 10_1$		1.1478	1.6469(199)	1.2204
$14_1 \rightarrow 12_1$		1.0390	1.2477(149)	1.1355
$16_1 \rightarrow 14_1$		0.8957	1.6966(349)	1.0188
$0_2 \rightarrow 2_1$	0.2550(392)	0.0853		0.1033
$2_2 \rightarrow 0_2$	0.4757(490)	0.5099		0.5025
$2_2 \rightarrow 0_1$	0.0042(3)	0.0042		0.0028
$2_2 \rightarrow 2_1$	0.0328(29)	0.0183		0.0226
$2_2 \rightarrow 4_1$	0.0961(78)	0.0490		0.0544
$4_2 \rightarrow 2_2$		0.7817		0.7872
$4_2 \rightarrow 2_1$		0.0025	0.0011(3)	0.0013
$4_2 \rightarrow 4_1$		0.0179	0.0648(199)	0.0233
$4_2 \rightarrow 6_1$		0.0398	0.0598(199)	0.0407
$6_2 \rightarrow 4_2$		0.8902	1.0430(1048)	0.9137
$6_2 \rightarrow 6_1$		0.0176	0.0558(54)	0.0243
$6_2 \rightarrow 4_1$		0.0010	0.0021(5)	0.0004
$8_2 \rightarrow 6_2$		0.9277	1.5471(1197)	0.9692
$8_2 \rightarrow 8_1$		0.0165	0.0399(4)	0.0241
$8_2 \rightarrow 6_1$		0.0004	0.0009(2)	0.0001
$10_2 \rightarrow 8_2$		0.9138	1.4970(149)	0.9749
$10_2 \rightarrow 10_1$		0.0146	0.0444(89)	0.0226
$10_2 \rightarrow 8_1$		0.0002	0.0019(3)	0.0000
$12_2 \rightarrow 10_2$		0.8550	0.7385(449)	0.9381
$12_2 \rightarrow 10_1$		0.0001	0.0015(2)	0.0000
$2_3 \rightarrow 0_2$	0.0059(12)	0.0013		0.0007
$2_3 \rightarrow 0_1$	0.0279(24)	0.0080	0.0359(39)	0.0163
$2_3 \rightarrow 2_1$	0.0603(49)	0.0103	0.0469(59)	0.0230
$2_3 \rightarrow 4_1$	0.0084(6)	0.0033	0.0628(94)	0.0060
$Q_{2_1}$	-1.82(4)	-1.813		-1.799

The  $B_{I+2/2}$  ratios of the B(E2) transition between the levels of yrast states for U(5) and SU(3) predictions are given by [31]

$$B_{I+2/2} = \frac{B(E2; I+2 \rightarrow I)}{B(E2; 2_1^+ \rightarrow 0_1^+)} = \begin{cases} \frac{1}{2}(I+2) \left(1 - \frac{I}{2N}\right) & \text{for U(5)} \\ \frac{15}{2} \frac{(I+2)(I+1)}{2(2I+3)(2I+5)} \left(1 - \frac{I}{2N}\right) \left(1 + \frac{I}{2N+3}\right) & \text{for SU(3)} \end{cases} \quad (7)$$

The  $B_{I+2/2}$  ratios, for the  $I_i = 0_1^+, 2_1^+, 4_1^+, 6_1^+$  and  $8_1^+$  levels, of the yrast band for  $^{150}\text{Nd}$ ,  $^{152}\text{Sm}$ ,  $^{154}\text{Gd}$ , and  $^{156}\text{Dy}$  isotones are presented in Tables 6-9 and also shown in Fig.5 along with the U(5), SU(3) and X(5) prediction.

Table 6. The experimental[30] and predicted  $B_{I+2/2}$  ratio of  $^{150}\text{Nd}$

$B_{I+2/2}$	Angular momentum I				
	0	2	4	6	8
Exp.	1	1.556(43)	1.774(123)	1.859(246)	1.730(139)
IBM-1	1	1.48	1.63	1.644	1.559
U(5)	1	1.777	2.333	2.666	2.777
X(5)	1	1.58	1.98	2.27	2.61
SU(3)	1	1.388	1.455	1.41	1.296

Table.7: The experimental[30] and predicted  $B_{I+2/2}$  ratio of  $^{152}\text{Sm}$

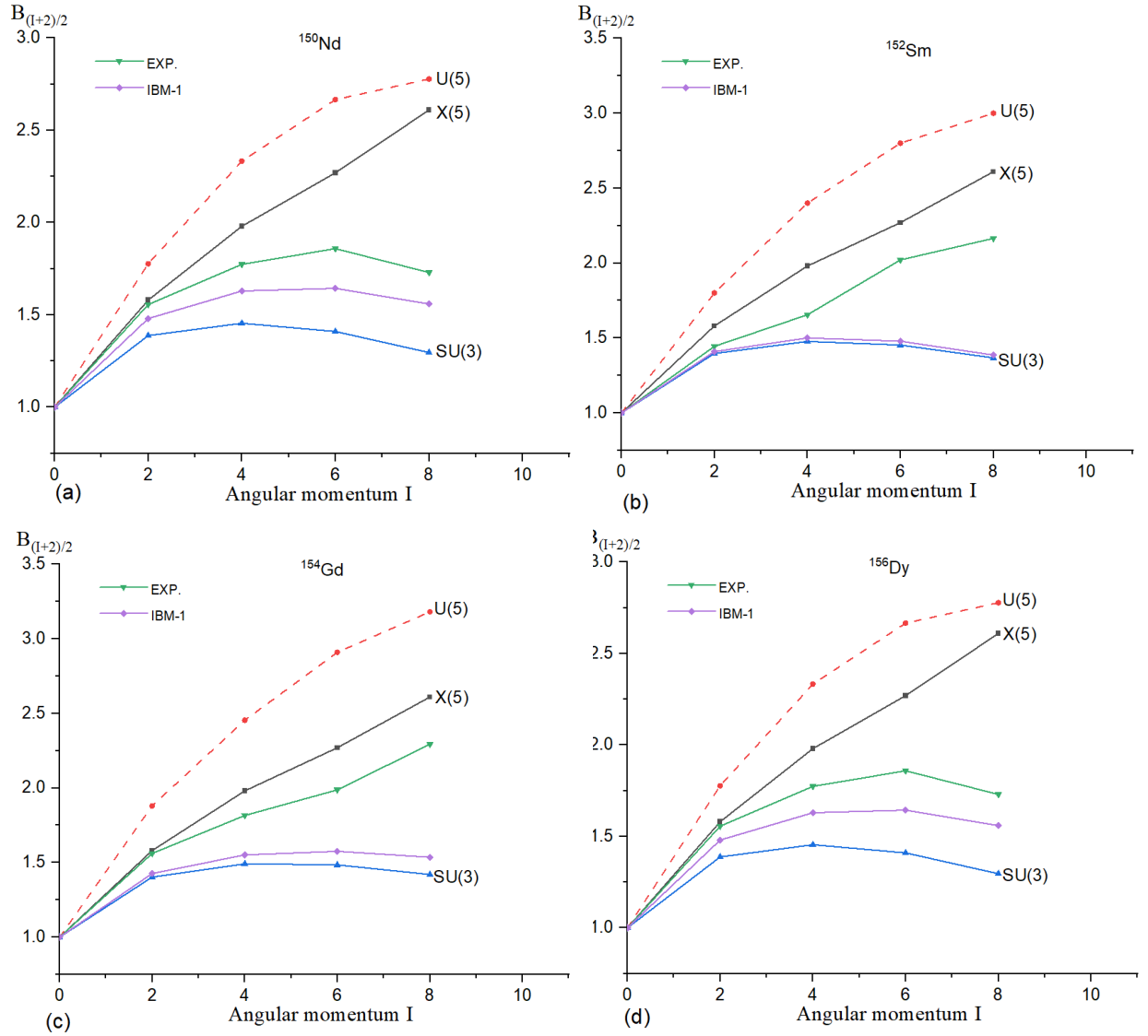
$B_{I+2/2}$	Angular momentum I				
	0	2	4	6	8
Exp.	1	1.444(174)	1.655(210)	2.021(250)	2.165(480)
IBM-1	1	1.409	1.500	1.478	1.386
U(5)	1	1.8	2.4	2.8	3
X(5)	1	1.58	1.98	2.27	2.61
SU(3)	1	1.397	1.477	1.453	1.367

Table 8: The experimental[30] and predicted  $B_{I+2/2}$  ratio of  $^{154}\text{Gd}$

$B_{I+2/2}$	Angular momentum I				
	0	2	4	6	8
Exp.	1	1.561(67)	1.815(107)	1.987(1095)	2.293(40)
IBM-1	1	1.426	1.551	1.575	1.535
U(5)	1	1.88	2.454	2.909	3.181
X(5)	1	1.58	1.98	2.27	2.61
SU(3)	1	1.402	1.491	1.484	1.419

Table.9: The experimental [30]and predicted  $B_{I+2/2}$  ratio of  $^{156}\text{Dy}$

$B_{I+2/2}$	Angular momentum I				
	0	2	4	6	8
Exp.	1	1.556(201)	1.774(289)	1.859(265)	1.730(254)
IBM-1	1	1.480	1.630	1.644	1.559
U(5)	1	1.777	2.333	2.666	2.777
X(5)	1	1.58	1.98	2.27	2.61
SU(3)	1	1.388	1.455	1.410	1.296



**Fig.5.** The predicted  $B(I+2)/2$  ratios for  $^{150}\text{Nd}$ - $^{156}\text{Dy}$  isotones in comparison to the experimental data.

The  $B(E2)$  ratio of interband transitions is another property used to test the nucleus shape and its limit. In Table 10, the values of the following ratios:-

$$\begin{aligned}
 R_1 &= \frac{B(E2;2_2 \rightarrow 0_1)}{B(E2;2_2 \rightarrow 2_1)}, R_2 = \frac{B(E2;2_2 \rightarrow 2_1)}{B(E2;2_1 \rightarrow 0_1)}, R_3 = \frac{B(E2;4_1 \rightarrow 2_1)}{B(E2;2_2 \rightarrow 2_1)} \\
 R_4 &= \frac{B(E2;3_1 \rightarrow 2_1)}{B(E2;3_1 \rightarrow 4_1)}, R_5 = \frac{B(E2;4_2 \rightarrow 4_1)}{B(E2;4_2 \rightarrow 2_2)}, R_6 = \frac{B(E2;4_1 \rightarrow 2_1)}{B(E2;2_1 \rightarrow 0_1)}
 \end{aligned} \quad (8)$$

for the isotones  $^{150}\text{Nd}$ ,  $^{152}\text{Sm}$ ,  $^{154}\text{Gd}$ , and  $^{156}\text{Dy}$  are compared to the typical values of the U(5), O(6), SU(3) and X(5) limits [11,32] in Table 10. It is clear from Fig. 5 and Tables 6-10 that these isotones have the U(5)-SU(3) transitional characters.

Table 10. The experimental [30] and theoretical B(E2) ratios in the Nd-Dy isotones

	B(E2) ratios	R <sub>1</sub>	R <sub>2</sub>	R <sub>3</sub>	R <sub>4</sub>	R <sub>5</sub>	R <sub>6</sub>
Isotones	U(5)	0.011	1.40	1.00	0.06	0.72	
	SU(3)	0.70	0.02	6.93	2.50	0.03	
	O(6)	0.07	0.79	1.84	0.12	0.75	
<sup>150</sup> Nd	X(5)						1.58
	Exp.	0.07(5)	0.09(2)	18.07(538)			1.55(4)
	IBM-1	0.04	0.12	12.45	0.80	0.13	1.48
<sup>152</sup> Sm	Exp.	0.16(12)	0.04(1)	36.85(1238)	1.06	0.02	1.44(17)
	IBM-1	0.16	0.012	118.25	0.11	0.01	1.41
<sup>154</sup> Gd	Exp.	0.13(1)	0.043(4)	36.64(351)			1.56(7)
	IBM-1	0.23	0.023	61.95	1.28	0.02	1.43
<sup>156</sup> Dy	Exp.						1.63(20)
	IBM-1	0.12	0.03	50.19	1.31	0.03	1.44

### 1.3. Potential Energy Surface (PES)

The potential energy surface (PES) is a useful property for describing the shape of complex systems containing multiple particles in a closed shell. The PES calculations are carried out in conjunction with the intrinsic part of the IBM Hamiltonian, which is dependent on the shape variables  $\beta$  and  $\gamma$ . The intrinsic ground state of the IBM-1 is given by[28]:

$$|N, \beta, \gamma\rangle = \frac{1}{\sqrt{N!}} (b_c^\dagger)^N |0\rangle \tag{9}$$

where  $N$  is the boson number,  $|0\rangle$  denotes the boson vacuum and  $b_c^\dagger$  is given by[28]:

$$b_c^\dagger = \frac{1}{\sqrt{1+\beta^2}} \left[ s^\dagger + \beta \left( \cos \gamma (d_0^\dagger) + \frac{1}{\sqrt{2}} \sin \gamma (d_2^\dagger + d_{-2}^\dagger) \right) \right] \tag{10}$$

The Potential Energy Surface is expressed in terms of the shape variables  $\beta$  and  $\gamma$  as follow [2]:

$$E(N, \beta, \gamma) = \frac{N}{1+\beta^2} + \frac{N(N-1)}{(1+\beta^2)^2} (\alpha_1 \beta^4 + \alpha_2 \beta^3 \cos 3\gamma + \alpha_3 \beta^2 + \alpha_4) \tag{11}$$

The nuclear surface geometry is determined by  $\beta$  and  $\gamma$ , and they take the value of  $\beta \geq 0$  and  $0 \leq \gamma \leq \pi/3$ .  $\beta_{min} = 0$  for spherical nuclei, , but not for deformable and  $\gamma$ -unstable nuclei [26]. When  $\gamma = 0^\circ$ , the distortion has a prolate shape, and when it equals  $60^\circ$ , the deformation has an oblate shape. Figure 6 shows contour plots of the potential energy surface of transitional deformed nuclei <sup>150</sup>Nd, <sup>152</sup>Sm, <sup>154</sup>Gd, and <sup>156</sup>Dy

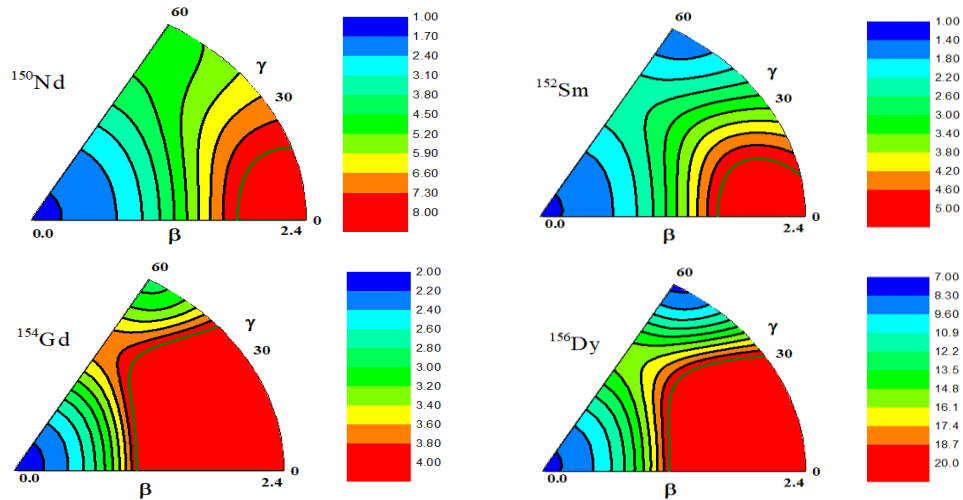


Fig. 6 The potential energy surfaces for  $^{150}\text{Nd}$ ,  $^{152}\text{Sm}$ ,  $^{154}\text{Gd}$ , and  $^{156}\text{Dy}$  isotones

## 2. Summary and Conclusion

In the framework of IBM-1 model, the energy levels and quadrupole transitional probabilities in  $^{150}\text{Nd}$ ,  $^{152}\text{Sm}$ ,  $^{154}\text{Gd}$ , and  $^{156}\text{Dy}$  isotones have been investigated. The values of the interaction parameters and the obtained results indicate that the Nd-Dy(N=90) isotones are close to the X(5) critical points, and the shape-phase transition from U(5) to SU(3) is observed. Further determination of this transitional structure for these isotones is obtained from the PES calculations. Comparing the theoretical results in this study with the available practical values shows the ability of the model to describe the nuclear properties of the selected nuclei.

## 3. References

- [1] F. Iachello et al., Nuclear structure. Pub.(Plenum, New York and London) Ed. Abrahams K., Allaart K., and Diapering AEL, 1981.
- [2] F. Iachello, A. Arima, Mod. Phys **59**, 339 (1987).
- [3] O. Scholten, The interacting boson approximation model and applications. 1980.
- [4] R. Casten, D. Warner, Reviews of Modern Physics **60**(2), 389 (1988). Doi: <https://doi.org/10.1103/RevModPhys.60.389>
- [5] P. Cejnar, J. Jolie, R.F. Casten, Reviews of Modern Physics **82**(3), 2155 (2010). Doi:<https://doi.org/10.1103/RevModPhys.82.2155>
- [6] A. Arima, F. Iachello, Annual Review of Nuclear and Particle Science **31**(1), 75 (1981).
- [7] A. Arima, F. Iachello, Annals of Physics **123**(2), 468 (1979). Doi: [https://doi.org/10.1016/0003-4916\(79\)90347-6](https://doi.org/10.1016/0003-4916(79)90347-6)
- [8] A. Arima, F. Iachello, Annals of Physics **111**(1), 201 (1978). Doi: [https://doi.org/10.1016/0003-4916\(78\)90228-2](https://doi.org/10.1016/0003-4916(78)90228-2)
- [9] A. Arima, F. Iachello, Annals of Physics **99**(2), 253 (1976). Doi:<https://doi.org/10.1006/aphy.2000.6007>
- [10] F. Iachello, Physical Review Letters **85**(17), 3580 (2000). Doi:<https://doi.org/10.1103/PhysRevLett.85.3580>
- [11] F. Iachello, Physical Review Letters **87**(5), 052502 (2001). Doi:<https://doi.org/10.1103/PhysRevLett.87.052502>
- [12] J. Gupta, Journal of Physics G: Nuclear and Particle Physics **21**(4), 565 (1995). Doi:<https://doi.org/10.1088/0954-3899/21/4/008>
- [13] L. Li-Jun, Z. Jin-Fu, Chinese Physics C **30**(2),128 (2006).
- [14] F. Sharrad et al., Armenian Journal of Physics **5**(3),111 (2012).
- [15] A. Khalaf, T. Awwad, Progress in Physics **1**, 7 (2013).
- [16] F. H. Al-Khudair et al, Commun. Theor. Phys **62**(6), 847 (2014). Doi:<https://doi.org/10.1088/0253-6102/62/6/12>

- [17] A.M. Khalaf, M.M. Taha, *Journal of Theoretical and Applied Physics* **9**(2), 127 (15).  
Doi:<https://doi.org/10.1007/s40094-015-0170-z>
- [18] J. Gupta, *Physical Review C* **92**(4), 044316 (2015).  
Doi:<https://doi.org/10.1103/PhysRevC.92.044316>
- [19] S.A. Eid, X. Diab, *PROGRESS* **12**,170 (2016).
- [20] S.Y. Lee, J. Lee, Y.J. Lee, *Journal of the Korean Physical Society* **72**, 1147 (2018).  
Doi:<https://doi.org/10.3938/jkps.72.1147>
- [21] H.N. Qasim, F.H. Al-Khudair, *International Journal of Modern Physics E* **28**(12) 1950107 (2019). Doi: <https://doi.org/10.1142/S0218301319501076>
- [22] H. Baoyue et al., *原子核物理评论* **38**(4), 368 (2021).  
Doi:<http://dx.doi.org/10.11804/NuclPhysRev.38.2021059>
- [23] E. Balbutsev et al., *Physical Review C* **105**(4), 044323 (2022).  
Doi:<https://doi.org/10.1103/PhysRevC.105.044323>
- [24] B. He, S. Zhang, L. Li, Y. Luo, Y. Zhang, F. Pan, et al, *Physical Review C* **105**(4), 044332 (2022). Doi:<https://doi.org/10.1103/PhysRevC.105.044332>
- [25] A. Arima, F. Iachello, Springer , 139 (1984). Doi:[https://doi.org/10.1007/978-1-4613-9892-9\\_2](https://doi.org/10.1007/978-1-4613-9892-9_2)
- [26] R.F. Casten, D.D. Warner, *Reviews of Modern Physics* **60**(2), 389 (1988).  
Doi:<https://doi.org/10.1103/RevModPhys.60.389>
- [27] F. Radhi, N. Stewart, *Zeitschrift für Physik A Hadrons and Nuclei* **356**(1), 145 (1996).  
Doi:<https://doi.org/10.1007/BF02769211>
- [28] A. Dieperink, O. Scholten, F. Iachello, *Physical Review Letters* **44**(2), 1747 (1980).  
Doi:<https://doi.org/10.1103/PhysRevLett.44.1747>
- [29] O. Scholten, Computer code PHINT, KVI. Groningen Holland (1980).
- [30] [www.nndc.bnl.gov/ensdf/2022](http://www.nndc.bnl.gov/ensdf/2022).
- [31] M. Kotb, *Physics of Particles and Nuclei Letters* **13**, 451 (2016).  
Doi:<https://doi.org/10.1134/S1547477116040075>
- [32] J. Stachel, P. Van Isacker, K. Heyde, *Physical review C* **25**(1), 650 (1982).  
Doi:<https://doi.org/10.1103/PhysRevC.25.650>

## الخاصية الانتقالية للآيسوتونات Nd-Dy (N=90) في نموذج IBM

عبدالله حسين عبدعلي، فهمي شعبان راضي\*

قسم الفيزياء، كلية التربية للعلوم الصرفة، جامعة البصرة، بصرة، العراق.

### الملخص

تم استخدام نموذج البوزونات المتفاعلة لدراسة تركيب مستويات الطاقة للحزم الأرضية، بيتا و كما في الآيسوتونات  $^{150}\text{Nd}$ ,  $^{152}\text{Sm}$ ,  $^{154}\text{Gd}$  and  $^{156}\text{Dy}$  (N = 90). قيم نسب الطاقة  $R_{0_2/2_1}$  و  $R_{I+2/2}$  تم مقارنتها مع التوقع النظري للتمائل  $U(5)$ ,  $SU(3)$  و  $X(5)$ . تمت مقارنة احتمالات الانتقال المختزل المحسوبة و كذلك العزوم الرباعية القطب مع البيانات العملية. نموذج IBM-1 بحث خواص سطح طاقة الجهد لتحديد الشكل النووي للآيسوتونات Nd-Dy (N=90).

### معلومات البحث

الاستلام 23 تموز 2023  
القبول 02 اب 2023  
النشر 30 كانون الأول 2023

### الكلمات المفتاحية

IBM-1 ، مستويات الطاقة ، B(E2)

**Citation:** A. H. Abd, F. S. Radhi ,J.  
Basrah Res. (Sci.) 49(2), 48  
(2023).DOI:  
<https://doi.org/10.56714/bjrs.49.2.5>

\*Corresponding author email : fahmishaban.fs@gmail.com

